Toxicology Letters 199 (2010) 225–233

Contents lists available at ScienceDirect

Toxicology Letters

journal homepage: www.elsevier.com/locate/toxlet

Mercury modulates the CYP1A1 at transcriptional and posttranslational levels in human hepatoma HepG2 cells

Issa E.A. Amara, Anwar Anwar-Mohamed, Ayman O.S. El-Kadi*

Faculty of Pharmacy and Pharmaceutical Sciences, University of Alberta, Edmonton, Alberta, Canada T6G 2N8

ARTICLE INFO

Article history:
Received 27 July 2010
Received in revised form 3 September 2010
Accepted 6 September 2010
Available online 15 September 2010

Keywords:
CYP1A1
Mercury
Dioxin
Heavy metals
Toxicity

ABSTRACT

Aryl hydrocarbon receptor (AhR) ligands such as 2,3,7,8-tetrachlorodibenzo-*p*-dioxin (TCDD) and metals, such as mercury (Hg^{2+}), are environmental co-contaminants and their molecular interaction may disrupt the coordinated regulation of the carcinogen-activating enzyme cytochrome P450 1A1 (CYP1A1). Therefore, we examined the effect of co-exposure to Hg^{2+} and TCDD on the expression of the CYP1A1 in HepG2 cells. Our results showed that Hg^{2+} significantly inhibited the TCDD-mediated induction of CYP1A1 at the mRNA, protein, and catalytic activity levels. At the transcriptional level, co-exposure to Hg^{2+} and TCDD significantly decreased the TCDD-mediated induction of AhR-dependent luciferase reporter gene expression. Moreover, Hg^{2+} did not affect CYP1A1 mRNA stability, while decreasing its protein half-life, suggesting the involvement of a posttranslational mechanism. Importantly, Hg^{2+} increased the expression of heme oxygenase-1 (HO-1), a rate limiting enzyme in heme degradation, which coincided with further decrease in the CYP1A1 catalytic activity levels. Upon using a competitive HO-1 inhibitor, tin mesoporphyrin, heme precursor, hemin, or transfecting the HepG2 cells with siRNA for HO-1 there was a partial restoration of the inhibition of TCDD-mediated induction of CYP1A1 catalytic activity. In conclusion, we demonstrate that Hg^{2+} down-regulates the expression of CYP1A1 at the transcriptional and posttranslational levels in HepG2 cells. In addition, HO-1 is involved in the modulation of CYP1A1 at the posttranslational level.

1. Introduction

Co-contamination of heavy metals, such as mercury (Hg^{2+}), with halogenated aromatic hydrocarbons (HAHs) such as 2,3,7,8-tetrachlorodibenzo-*p*-dioxin (TCDD), is a common environmental problem with multiple biological consequences. Hg^{2+} is mostly considered highly toxic agent that is introduced into the environment through natural and/or industrial sources (Snow et al., 1989). Both aryl hydrocarbon receptor (AhR) ligands and heavy metals are ranked high on the list of the most hazardous xenobiotics in the environment, as reported by the Agency for Toxic Substances and Diseases Registry and the Canadian Environmental Protection Act. (ATSDR, 2005; CEPA, 2006). Studies on the carcinogenicity and mutagenicity of HAHs have demonstrated the role of cytochrome P450 1A1 (CYP1A1), a phase I xenobiotics-metabolizing enzyme, in bioactivating poly aromatic hydrocarbons (PAHs) to epoxide and diol-epoxide intermediates, which will subsequently lead to DNA and protein adducts formation (Shimada and Fujii-Kuriyama, 2004).

The AhR is a ligand-activated cytoplasmic transcription factor that belongs to the basic-helix-loop-helix protein family. The AhR plays a key role in the regulation of CYP1A1. This cytosolic inactive receptor exists attached to a complex of two heat shock proteins 90 (HSP90), hepatitis B virus X-associated protein (XAP2), and the chaperone protein p23 (Hankinson, 1995; Meyer et al., 1998). Upon ligand binding, the activated AhR dissociates from the cytoplasmic complex, and translocates to the nucleus where it dimerizes with the aryl hydrocarbon nuclear translocator (Arnt) (Whitelaw et al., 1994). Thereafter, the ligand/AhR/Arnt complex acts as a transcription factor that binds to a specific DNA recognition sequence, GCGTG, within the xenobiotic responsive element (XRE), located in the promoter region of a battery of genes termed AhR-regulated genes such as CYP1A1 (Denison et al., 1989; Nebert et al., 2004). The toxicological effects of HAHs, typified by TCDD, are mainly mediated through the activation of AhR and consequently CYP1A1. In fact, a strong correlation between the induction of CYP1A1 and cancer has been previously reported (McLemore et al., 1990).

The majority of published studies on AhR ligands toxicities have been conducted individually, yet human exposures are usually to

* Corresponding author at: Faculty of Pharmacy & Pharmaceutical Sciences, 3126 Dentistry/Pharmacy Centre, University of Alberta, Edmonton, Alberta, Canada T6G 2N8. Tel.: +1 780 492 3071; fax: +1 780 492 1217.
E-mail address: aelkadi@pharmacy.ualberta.ca (A.O.S. El-Kadi).

0378-4274/$ – see front matter © 2010 Elsevier Ireland Ltd. All rights reserved.
doi:10.1016/j.toxlet.2010.09.003

mixtures of these ligands and metals such as Hg^{2+}. Hg^{2+} is a metal that is widely used in the foundry, mining, and manufacturing industries and is a component in a number of electrical instruments and medical products such as thermometers, thermostats, dental amalgams, switches, and batteries (Gochfeld, 2003). Among metals, Hg^{2+} is unique in that it is found in the environment in several physical and chemical forms. At room temperature, elemental (or metallic) Hg^{2+} exists as a liquid (Zalups, 2000). As a result of its high vapor pressure, this form of Hg^{2+} is released into the environment as Hg^{2+} vapor. Hg also exists in three different oxidation states such as Hg^0, which exists in metallic form as vapor, and Hg^+ or Hg^{2+}, which can form stable organic compound such as methylmercury. Generally, the route and efficiency of exposure depends mainly on the oxidation state of Hg (Ercal et al., 2001; Tezel et al., 2001).

Previous reports from our laboratory and others have demonstrated that Hg^{2+} alters the expression of the carcinogen-activating enzyme CYP1A1, at different signaling pathway levels (Korashy and El-Kadi, 2004; Vakharia et al., 2001). Therefore, the objective of this study was to determine the possible effects of Hg^{2+} on the TCDD-mediated induction of CYP1A1, and to investigate the underlying molecular mechanisms involved in this pathway.

We provide here the evidence that Hg^{2+} modulates the expression of CYP1A1 through affecting its transcriptional and posttranslational levels. The inhibitory effect of Hg^{2+} on the TCDD-mediated induction of CYP1A1 catalytic activity might be in part due to its effect on HO-1, which will subsequently lead to the formation of a hollow functionless CYP1A1 protein. Furthermore, Hg^{2+} significantly alters the expression of CYP1A1 protein stability, suggesting posttranslational down-regulation of CYP1A1 by Hg^{2+}.

2. Materials and methods

2.1. Materials

3-(4,5-Dimethylthiazol-2-yl)-2,5-diphenyltetrazolium bromide (MTT), cycloheximide (CHX), 7-ethoxyresorufin, fluorescamine, anti-goat IgG peroxidase secondary antibody, hemin, protease inhibitor cocktail, and mercuric chloride ($HgCl_2$) were purchased from Sigma Chemical Co. (St. Louis, MO). Tin mesoporphyrin (SnMP), was purchased from Frontier Scientific Inc. (Logan, UT). TCDD, >99% pure, was purchased from Cambridge Isotope Laboratories (Woburn, MA). TRIzol reagent and Lipofectamine 2000 reagents were purchased from Invitrogen (San Diego, CA). High-Capacity cDNA Reverse Transcription Kit, SYBR® Green PCR Master Mix, human Hmox1 (HO-1) validated siRNA was purchased from Applied Biosystems (Foster City, CA). INTERFERin siRNA transfecting reagent was purchased from Polyplus transfection (Illkirch, France). Actinomycin-D (Act-D) was purchased from Calbiochem (San Diego, CA). Chemiluminescence Western blotting detection reagents were from GE Healthcare Life Sciences (Piscataway, NJ). Nitrocellulose membrane was purchased from Bio-Rad Laboratories (Hercules, CA). CYP1A1 mouse polyclonal primary antibody, GAPDH rabbit polyclonal antibody, and anti-rabbit IgG peroxidase secondary antibody were purchased from Santa Cruz Biotechnology, Inc. (Santa Cruz, CA). Anti-mouse IgG peroxidase secondary antibody was purchased from R&D Systems, Inc. (Minneapolis, MN). Luciferase assay reagents were obtained from Promega (Madison, WI). All other chemicals were purchased from Fisher Scientific (Toronto, ON).

2.2. Cell culture

HepG2 cell line, ATCC number HB-8065 (Manassas, VA), were maintained in Dulbecco's modified Eagle's medium (DMEM) with phenol red, supplemented with 10% heat-inactivated fetal bovine serum, 20 μM l-glutamine, 50 μg/ml amikacin, 100 IU/ml penicillin, 10 μg/ml streptomycin, 25 ng/ml amphotericin B, 0.1 mM non-essential amino acids, and vitamin supplement solution. Cells were grown in 75-cm^2 cell culture flasks at 37 °C in a 5% CO_2 humidified incubator.

2.3. Chemical treatments

Cells were treated in serum free medium with various concentrations of Hg^{2+} (2.5–10 μM) in the absence and presence of 1 nM TCDD, and/or 5 μM SnMP and 80 μM hemin as described in figure legends. TCDD and SnMP were dissolved in dimethylsulfoxide (DMSO) and maintained in DMSO at −20 °C until use. Hg^{2+} and hemin (10 mM stocks) were prepared freshly in double de-ionized water. In all treatments, the DMSO concentration did not exceed 0.05% (v/v).

2.4. Effect of Hg^{2+} on cell viability

The effect of Hg^{2+} on cell viability was determined using the MTT assay as described previously (Anwar-Mohamed and El-Kadi, 2009). MTT assay measures the conversion of MTT to formazan in living cells via mitochondrial enzymes of viable cells. In brief, HepG2 cells were seeded onto 96-well microtiter cell culture plates and incubated for 24 h at 37 °C in a 5% CO_2 humidified incubator. Cells were treated with various concentrations of Hg^{2+} (2.5–50 μM) in the absence and presence of 1 nM TCDD. After 24 h incubation, the medium was removed and replaced with cell culture medium containing 1.2 mM MTT dissolved in phosphate buffered saline (PBS) (pH 7.4). After 2 h of incubation, the formed crystals were dissolved in isopropanol. The intensity of the color in each well was measured at a wavelength of 550 nm using the Bio-Tek EL 312e microplate reader (Bio-Tek Instruments, Winooski, VT).

2.5. RNA extraction and quantitative real-time PCR

After incubation with the test compounds for the specified time periods, total cellular RNA was isolated using TRIzol reagent, according to manufacturer's instructions (Invitrogen), and quantified by measuring the absorbance at 260 nm. For reverse transcription-polymerase chain reaction (RT-PCR), first-strand cDNA was synthesized from 1.0 μg of total RNA using the High-Capacity cDNA Reverse Transcription Kit with random primers. Real-time PCR reactions were performed on an ABI 7500 real-time PCR system (Applied Biosystems), using SYBR® Green PCR Master Mix (Applied Biosystems). The amplification reactions were performed as follows: 10 min at 95 °C, and 40 cycles of 94 °C for 15 s and 60 °C for 1 min. Primers and probes for human CYP1A1 were: Forward primer 5′-CTA TCT GGG CTG TGG GCA A-3′, reverse primer 5′-CTG GCT CAA GCA CAA CTT GG-3′. Heme oxygenase-1 (HO-1): forward primer 5′-ATG GCC TCC CTG TAC CAC ATC-3′, reverse primer 5′-TGT TGC GCT CAA TCT CCT CCT-3′ and for β-actin: forward primer 5′-CTG GCA CCC AGG ACA ATG-3′, reverse primer 5′-GCC GAT CCA CAC GGA GTA-3′ were purchased from Integrated DNA technologies (IDT, Coralville, IA). The fold change in the level of *CYP1A1* or *HO-1* (target genes) between treated and untreated cells, corrected by the level of β-actin, was determined using the following equation: fold change = $2^{-\Delta(\Delta Ct)}$, where $\Delta Ct = Ct_{(target)} - Ct_{(\beta\text{-actin})}$ and $\Delta(\Delta Ct) = \Delta Ct_{(treated)} - \Delta Ct_{(untreated)}$.

2.6. Protein extraction and Western blot analysis

Twenty-four hours after incubation with the test compounds, cells were collected in lysis buffer containing 50 mM HEPES, 0.5 M sodium chloride, 1.5 mM magnesium chloride, 1 mM EDTA, 10% (v/v) glycerol, 1% Triton X-100, and 5 μl/ml of protease inhibitor cocktail. The cell homogenates were obtained by incubating the cell lysates on ice for 1 h, with intermittent vortexing every 10 min, followed by centrifugation at 12,000 × *g* for 10 min at 4 °C. Proteins (50 μg) were resolved by denaturing gel electrophoresis, as described previously (Elbekai and El-Kadi, 2004). Briefly, the cell homogenates were dissolved in 1X sample buffer, boiled for 5 min, separated by 10% SDS-PAGE and electrophoretically transferred to a nitrocellulose membrane. Protein blots were blocked for 24 h at 4 °C in blocking buffer containing 5% skim milk powder, 2% bovine serum albumin and 0.05% (v/v) Tween-20 in tris-buffered saline solution (TBS; 0.15 M sodium chloride, 3 mM potassium chloride, 25 mM Tris–base). After blocking, the blots were incubated with a primary polyclonal mouse anti-rat CYP1A1 antibody for 2 h at room temperature, and primary polyclonal rabbit anti-human GAPDH antibody for overnight at 4 °C in TBS containing 0.05% (v/v) Tween-20 and 0.02% sodium azide. Incubation with a peroxidase-conjugated anti-mouse IgG secondary antibody for CYP1A1 and anti-rabbit for GAPDH was carried out in blocking buffer for 1 h at room temperature. The bands were visualized with the enhanced chemiluminescence method according to manufacturer's instructions (GE Healthcare Life Sciences, Piscataway, NJ). The intensity of CYP1A1 protein bands was quantified, relative to the signals obtained for GAPDH protein, using ImageJ software.

2.7. Determination of CYP1A1 enzymatic activity

CYP1A1-dependent 7-ethoxyresorufin O-deethylase (EROD) was performed on intact living cells using 7-ethoxyresorufin as previously described (Anwar-Mohamed et al., 2008). Enzymatic activity was normalized for cellular protein content, which was determined using a modified fluorescent assay (Lorenzen and Kennedy, 1993).

2.8. Transient transfection and luciferase assay

HepG2 cells were plated onto 12-well cell culture plates. Each well of cells was transfected with 1.6 μg of XRE-driven luciferase reporter plasmid pGudLuc 6.1, generously provided by Dr. M.S. Denison (University of California, Davies), using lipofectamine 2000 reagent according to manufacturer's instructions (Invitrogen). Luciferase assay was performed according to manufacturer's instructions (Promega) as described previously (Elbekai and El-Kadi, 2007). Briefly, after incubation with test compounds for 24 h, cells were washed with PBS and a 200 μl of 1× lysis buffer was added into each well with continuous shaking for at least 20 min, then the content of each well was collected separately in 1.5 ml microcentrifuge tubes. Luciferase activities were analyzed in 100-μl cell extracts with the Luciferase Assay

System (Promega) on a TD-20/20 luminometer (Turner BioSystems, Sunnyvale CA). Luciferase activity is reported as emitted light per well as a percent of control, vehicle treated cells.

2.9. CYP1A1 mRNA stability

The half-life of CYP1A1 mRNA was analyzed by an Act-D-chase assay. Cells were pre-treated with 1 nM TCDD for 12 h. Cells were then washed and incubated with 5 μg/ml Act-D, to inhibit further RNA synthesis, immediately before treatment with Hg^{2+} (10 μM). Total RNA was extracted at 0, 1, 3, 6, and 12 h after incubation with Hg^{2+}. The fold change in the level of *CYP1A1* (target gene) between treated and untreated cells, corrected by the level of β-actin, was determined using the following equation: fold change = $2^{-\Delta(\Delta Ct)}$, where $\Delta Ct = Ct_{(target)} - Ct_{(\beta\text{-actin})}$ and $\Delta(\Delta Ct) = \Delta Ct_{(treated)} - \Delta Ct_{(untreated)}$.

2.10. CYP1A1 protein stability

The half-life of CYP1A1 protein was analyzed by CHX-chase assay. Cells were pre-treated with 1 nM TCDD for 24 h. Cells were then washed and incubated with 10 μg/ml CHX, to inhibit further protein synthesis, immediately before treatment with Hg^{2+}. Cells were collected in lysis buffer containing 50 mM HEPES, 0.5 M sodium chloride, 1.5 mM magnesium chloride, 1 mM EDTA, 10% (v/v) glycerol, 1% Triton X-100, and 5 μl/ml of protease inhibitor cocktail, at 0, 1,3, 6, 12, and 24 h after incubation with the metal. The cytosolic fractions were obtained by incubating the cell lysates on ice for 1 h, with intermittent vortexing every 10 min, followed by centrifugation at 12,000 × *g* for 10 min at 4 °C. Proteins (50 μg) were separated by 10% SDS-PAGE bis-acrylamide gel electrophoresis and electrophoretically transferred to a nitrocellulose membrane as described previously (Elbekai and El-Kadi, 2004). After blocking overnight in blocking buffer, protein blots were incubated with a primary polyclonal goat anti-human CYP1A1 antibody for 2 h at room temperature. Incubation with a peroxidase-conjugated rabbit anti-goat IgG secondary antibody was then carried out in blocking buffer for 1 h at room temperature. The bands were visualized with the enhanced chemiluminescence method according to manufacturer's instructions (GE Healthcare Life Sciences). Band densities were also then quantified using the ImageJ image processing program and the protein half-life values were determined from semilog plots of integrated densities versus time.

2.11. Transfecting HepG2 with HO-1 siRNA

HepG2 cells were plated onto 24-well cell culture plates. Each well of cells was transfected with HO-1 siRNA at the concentration of 20 nM using INTERFERin reagent according to manufacturer's instructions (Polyplus). HO-1 siRNA sequences were sense: CAA AUG CAG UAU UUU UGU Utt, and antisense: AAC AAA AAU ACU GCA UUU Gag. Transfection efficiency was determined using real-time PCR to detect HO-1 mRNA posttransfection at 6, 12, and 24 h. Therefore, cells were treated 6 h posttransfection with TCDD in the absence and presence of Hg^{2+} (10 μM) for 6 h to determine HO-1 and CYP1A1 mRNA levels, or 24 h to determine CYP1A1 catalytic activity levels.

2.12. Statistical analysis

The comparative analysis of the results from various experimental groups with their corresponding controls was performed using SigmaStat for Windows (Systat Software, Inc., CA). A *t*-test was carried out to assess statistical significance between control and TCDD treatments. Thereafter, a one-way analysis of variance (ANOVA) followed by Dunnett test was carried out to assess statistical significance between treatment groups compared to TCDD. For mRNA and protein half-lives statistical significance was assessed using two-way ANOVA followed by Dunnett test. The differences were considered significant when $P < 0.05$.

3. Results

3.1. Effect of co-exposure to Hg^{2+} and TCDD on cell viability

To determine the non-toxic concentrations of Hg^{2+} to be utilized in the current study, HepG2 cells were exposed for 24 h with increasing concentrations of Hg^{2+} (2.5–50 μM) in the absence and presence of 1 nM TCDD, thereafter cytotoxicity was assessed using the MTT assay. Fig. 1 shows that Hg^{2+} at concentrations of 2.5–25 μM in the presence and absence of 1 nM TCDD did not affect cell viability. However, the highest concentration tested (50 μM), significantly reduced the cell viability by 15% (Fig. 1). Therefore, all subsequent studies were conducted using the concentrations of 2.5–10 μM.

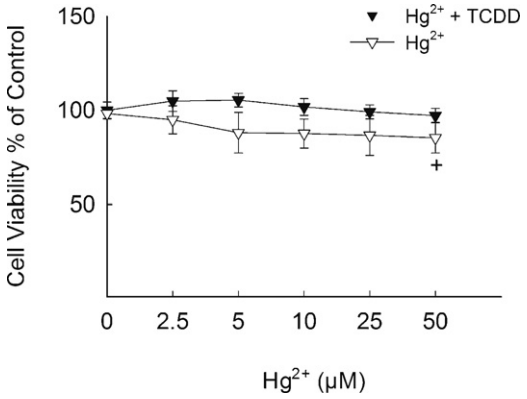

Fig. 1. Effect of Hg^{2+} on cell viability. HepG2 cells were treated for 24 h with Hg^{2+} (2.5–50 μM) in the absence and presence of 1 nM TCDD. Cell cytotoxicity was determined using MTT assay. Data are expressed as percentage of untreated control (which is set at 100%) ± SE ($n = 8$). (+) $P < 0.05$, compared to control (concentration = 0 μM); (*) $P < 0.05$, compared to respective TCDD treatment.

3.2. Concentration-dependent effect of co-exposure to Hg^{2+} and TCDD on inducible CYP1A1 mRNA

To examine the effect of co-exposure to Hg^{2+} and TCDD on CYP1A1 mRNA, HepG2 cells were treated with various concentrations of Hg^{2+} (2.5–10 μM) in the presence of 1 nM TCDD (Fig. 2). Thereafter, CYP1A1 mRNA was assessed using real-time PCR. Our results show that TCDD alone caused a significant increase of CYP1A1 mRNA by 43-fold, that was non-significantly inhibited by Hg^{2+} at the concentration of 2.5 and 5 μM, while the significant inhibition took place with the highest concentration tested, 10 μM. 10 μM Hg^{2+} significantly decreased the TCDD-mediated induction of CYP1A1 mRNA to 16-fold compared to TCDD alone (Fig. 2).

3.3. Concentration-dependent effect of co-exposure to Hg^{2+} and TCDD on CYP1A1 protein and catalytic activity

To investigate whether the observed inhibition of the TCDD-mediated induction of CYP1A1 mRNA by Hg^{2+} is further translated to the protein and catalytic activity levels, HepG2 cells were treated for 24 h with increasing concentrations of Hg^{2+} (2.5–10 μM) in the presence of 1 nM TCDD. Fig. 3A shows that TCDD alone caused a

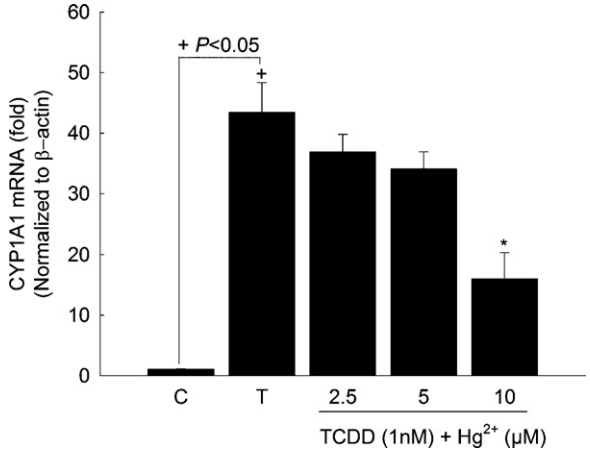

Fig. 2. Effect of Hg^{2+} on CYP1A1 mRNA using real-time PCR. HepG2 cells were treated with increasing concentrations of Hg^{2+} in the presence of 1 nM TCDD for 6 h. First-strand cDNA was synthesized from total RNA (1 μg) extracted from HepG2 cells. cDNA fragments were amplified and quantitated using ABI 7500 real-time PCR system as described under Section 2. Duplicate reactions were performed for each experiment, and the values presented are the means of six independent experiments ± SE ($n = 6$). (+) $P < 0.05$, compared to control (C) (concentration = 0 μM); (*) $P < 0.05$, compared to respective TCDD (T) treatment.

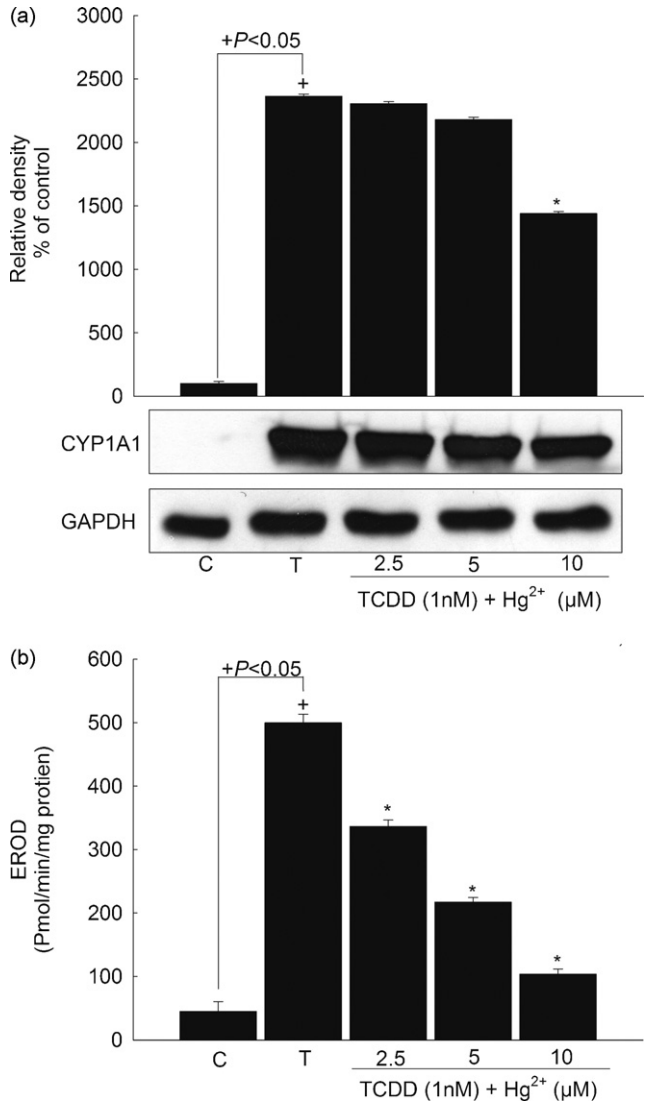

Fig. 3. Effect of Hg^{2+} on CYP1A1 protein and EROD activity. HepG2 cells were treated for 24 h with increasing concentrations of Hg^{2+} in the presence of 1 nM TCDD. (A) Protein (50 μg) was separated on a 10% SDS-PAGE and transferred to nitrocellulose membrane. Protein blots were then blocked overnight at 4 °C and then incubated with a primary CYP1A1 antibody for 2 h at room temperature, followed by 1 h incubation with secondary antibody at room temperature. CYP1A1 protein was detected using the enhanced chemiluminescence method. The intensity of bands was normalized to GAPDH signals, which was used as loading control. One of the three representative experiments is shown. (B) EROD activity was measured in intact living cells treated with increasing concentrations of Hg^{2+}, in the absence and presence of 1 nM TCDD for 24 h. CYP1A1 activity was measured using 7-ethoxyresorufin as a substrate. Values are presented as mean ± SE ($n = 6$). (+) $P < 0.05$, compared to control (C); (*) $P < 0.05$, compared to respective TCDD (T) treatment.

24-fold increase in CYP1A1 protein level. In agreement with the CYP1A1 mRNA results, Hg^{2+} at the concentration of 10 μM significantly decreased the TCDD-mediated induction of CYP1A1 protein to ~14-fold compared to TCDD alone. In addition, TCDD alone significantly increased CYP1A1 activity by approximately 11-fold. However, Hg^{2+} decreased the TCDD-mediated induction of CYP1A1 catalytic activity level in a concentration-dependent manner to 7.5-, 5- and 2-fold with Hg^{2+} concentrations of 2.5, 5, and 10, μM, respectively, compared to control (Fig. 3B).

3.4. Transcriptional inhibition of CYP1A1 gene by Hg^{2+}

In order to understand whether or not the inhibitory effect of Hg^{2+} on TCDD-mediated induction of CYP1A1 mRNA is actually due to a transcriptional mechanism, HepG2 cells were transiently transfected with the XRE-driven luciferase reporter gene. Luciferase activity results showed that 10 μM Hg^{2+} alone inhibited the constitutive expression of the luciferase activity to 0.7-fold compared to control (Fig. 4). On the other hand, 1 nM TCDD alone caused a significant increase in the luciferase activity by 60-fold compared to control. Interestingly, co-treatment with Hg^{2+} and TCDD significantly decreased the TCDD-mediated induction of luciferase activity to 34-fold compared to TCDD alone (Fig. 4).

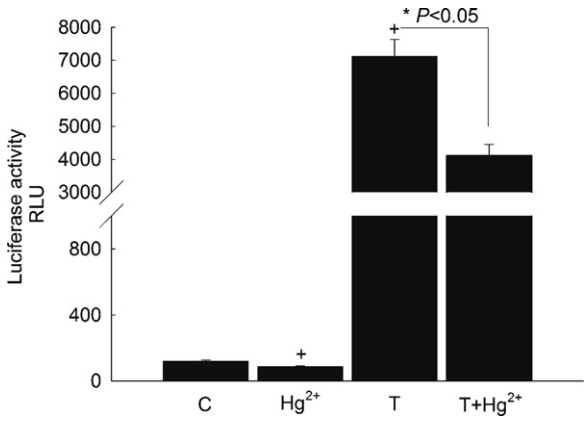

Fig. 4. Effect of Hg^{2+} on luciferase activity. HepG2 cells were transiently transfected with the XRE-luciferase transporter plasmid pGudLuc 6.1. Cells were treated with vehicle, TCDD (1 nM), Hg^{2+} (10 μM), TCDD (1 nM) + Hg^{2+} (10 μM) for 24 h. Cells were lysed and luciferase activity was measured according to manufacturer's instruction. Luciferase activity is reported as relative light unit. Values are presented as mean ± SE ($n = 6$). (+) $P < 0.05$, compared to control (C); (*) $P < 0.05$, compared to respective TCDD (T) treatment.

3.5. Posttranscriptional modification of CYP1A1 mRNA by Hg^{2+}

Although a transcriptional mechanism is involved in the Hg^{2+}-mediated down-regulation of the TCDD-mediated induction of CYP1A1 mRNA levels, there was still a possibility that a post-transcriptional mechanism might be involved. The level of mRNA expression is not only a function of the transcription rate, but is also dependent on the elimination rate, through processing or degradation. If Hg^{2+} decreases CYP1A1 mRNA via decreasing its stability, a decrease in half-life would be expected to take place. To examine the effect of Hg^{2+} on the CYP1A1 mRNA stability, we performed the Act-D chase experiment on intact viable HepG2 cells. Fig. 5 shows that CYP1A1 mRNA decayed with a half-life of 5.57 ± 0.99 h. Furthermore, Hg^{2+} did not significantly alter the CYP1A1 mRNA half-life which was 7.14 ± 0.95 h (Fig. 5).

3.6. Posttranslational modification of CYP1A1 protein by Hg^{2+}

The fact that Hg^{2+} inhibited the TCDD-mediated induction of CYP1A1 catalytic activity much more than what is observed at the mRNA levels raised the question of whether Hg^{2+} could modify CYP1A1 protein stability. Therefore, we measured the effect of Hg^{2+} on CYP1A1 protein half-life using CHX-chase experiment. Fig. 6 shows that CYP1A1 protein induced by TCDD degraded with a half-life of 10.78 ± 0.61 h. Interestingly, Hg^{2+} significantly decreased the stability of CYP1A1 protein which degraded with a half-life of 4.75 ± 0.81 h (Fig. 6).

3.7. Effect of co-exposure to Hg^{2+} and TCDD on HO-1 mRNA

The inverse relation between HO-1 expression and CYP1A1 activity directed us to probe the role of Hg^{2+} in inhibiting the TCDD-mediated induction of CYP1A1 at the catalytic activity level.

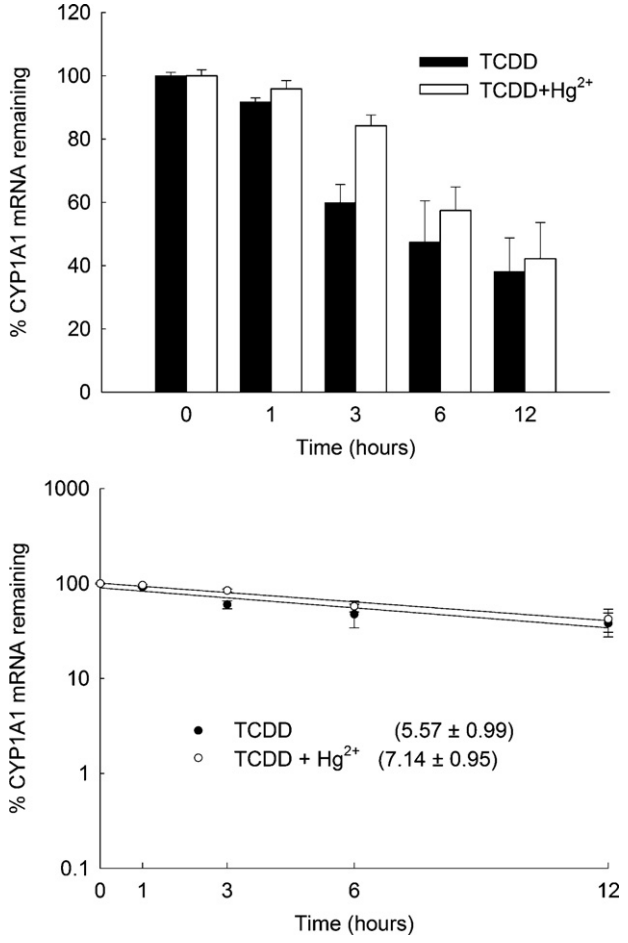

Fig. 5. Effect of Hg^{2+} on CYP1A1 mRNA half-life using real-time PCR. HepG2 cells were grown to 90% confluence in six-well cell culture plates, and then treated with 1 nM TCDD for 12 h. The cells were then washed and incubated in a fresh media containing 10 μM Hg^{2+} plus 5 μg/ml Act-D, a RNA synthesis inhibitor. First-strand cDNA was synthesized from total RNA (1 μg) extracted from HepG2 cells. cDNA fragments were amplified and quantitated using ABI 7500 real-time PCR system as described under Materials and Methods. Duplicate reactions were performed for each experiment, and the values presented are the means of six independent experiments. mRNA decay curves were analyzed individually, and the half-life was estimated from the slope of a straight line fitted by linear regression analysis ($r^2 \geq 0.81$) to a semilog plot of mRNA amount, expressed as a percent of treatment at time = 0 h (maximum, 100%) level, versus time. The half-lives obtained from six independent experiments were then used to calculate the mean half-life (mean ± SE, $n = 6$).

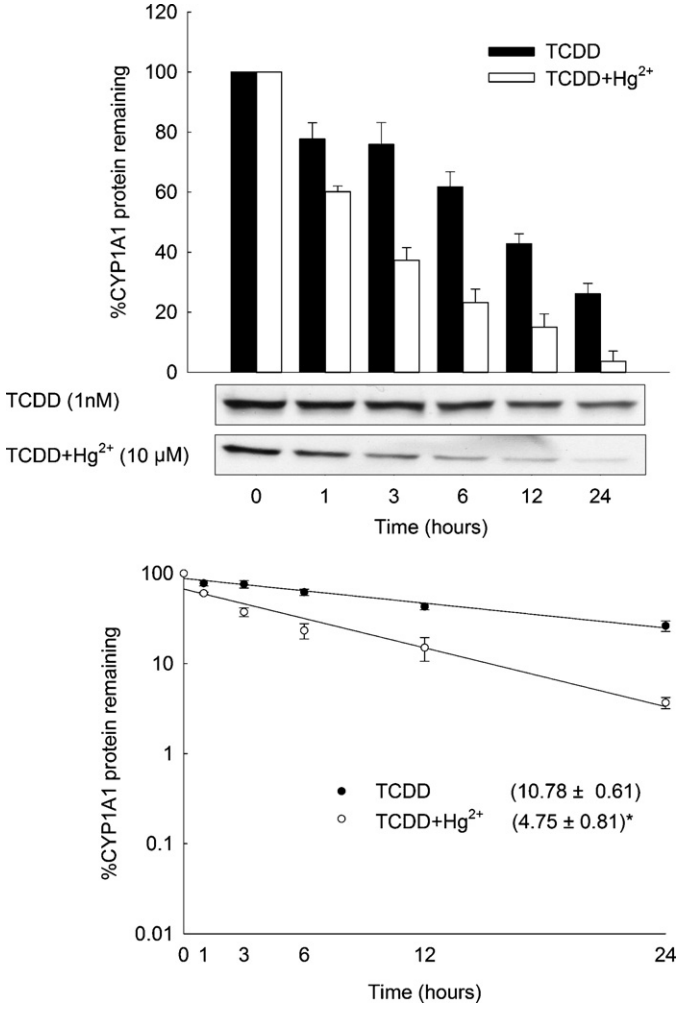

Fig. 6. Effect of Hg^{2+} on the CYP1A1 protein half-life. HepG2 cells were grown to 90% confluence in six-well cell culture plates. Thereafter, the cells were treated with 1 nM TCDD for 24 h. Cells were washed and incubated in fresh media containing 10 μM Hg^{2+} plus 10 μg/ml CHX, a protein translation inhibitor. Total cellular protein was extracted at the designated time points after the addition of CHX. Protein (50 μg) was separated by 10% SDS-PAGE and transferred to a nitrocellulose membrane. The intensities of CYP1A1 protein bands were normalized to GAPDH signals, which were used as loading controls. All protein decay curves were analyzed individually. The half-life was estimated from the slope of a straight line fitted by linear regression analysis to a semilog plot of protein amount, expressed as a percentage of treatment at time = 0 h (maximum, 100%) level, versus time. The half-lives obtained from three independent experiments were then used to calculate the mean half-life (mean ± SE, $n = 3$). (*) $P < 0.05$ compared with TCDD.

Therefore, we examined the effect of Hg^{2+} on HO-1 mRNA, a rate-limiting enzyme of heme degradation. For this purpose, HepG2 cells were treated with increasing concentrations of Hg^{2+} (2.5–10 μM) in the presence of 1 nM TCDD. Thereafter, HO-1 mRNA was measured using real-time PCR. Fig. 7 shows that TCDD alone did not alter HO-1 mRNA level. Whereas, co-exposure to TCDD and Hg^{2+} significantly increased the HO-1 mRNA level by 4.5-, 8-, and, 22-fold with concentrations of 2.5, 5, and 10 μM, respectively. Thus, HO-1 might be participating in the Hg^{2+}-mediated decrease of the TCDD-mediated induction of CYP1A1 at the catalytic activity (Fig. 7).

3.8. The effect of SnMP as a competitive inhibitor of HO-1 on the posttranslational modification of CYP1A1 catalytic activity by Hg^{2+}

To confirm the role of HO-1 in Hg^{2+}-mediated decrease of the TCDD-mediated induction of CYP1A1 catalytic activity, we examined the effect of HO-1 inhibitor, SnMP, on the decrease of CYP1A1 catalytic activity-mediated by Hg^{2+}. For this purpose HepG2 cells were co-exposed to 10 μM Hg^{2+} and 1 nM TCDD in the presence and absence of 5 μM SnMP. SnMP alone or in the presence of TCDD or Hg^{2+} plus TCDD did not affect CYP1A1 mRNA levels at all treatments, thus eliminating the possibility that SnMP reverses the inhibitory effect of Hg^{2+} on CYP1A1 catalytic activity through affecting its mRNA levels (Fig. 8A). Similarly, SnMP alone or in the presence of TCDD did not alter the CYP1A1 catalytic activity. TCDD alone increased the CYP1A1 catalytic activity by ~11-fold. On the other hand, Hg^{2+} at the concentration of 10 μM decreased the TCDD-mediated induction of CYP1A1 catalytic activity to ~5-fold compared to control (Fig. 8B). Intriguingly, SnMP partially reversed the Hg^{2+}-mediated decrease of CYP1A1 activity to reach ~9-fold compared to control. In spite of being successful in partially reversing the Hg^{2+}-mediated decrease of CYP1A1 activity through inhibiting HO-1, SnMP was unable to completely restore the CYP1A1 activity.

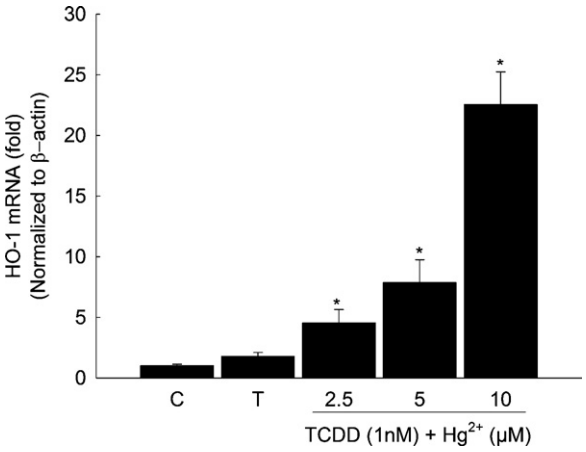

Fig. 7. Effect of Hg^{2+} on HO-1 mRNA. HepG2 cells were treated for 6 h with increasing concentrations of Hg^{2+} in the presence of 1 nM TCDD. First-strand cDNA was synthesized from total RNA (1 μg) extracted from HepG2 cells. cDNA fragments were amplified and quantitated using ABI 7500 real-time PCR system as described under Section 2. Duplicate reactions were performed for each experiment, and the values presented are the means of six independent experiments ± SE ($n = 6$). (+) $P < 0.05$, compared with control (C); (*) $P < 0.05$, compared with the respective TCDD (T) treatment.

3.9. The effect of exogenous heme on Hg^{2+}-mediated decrease of CYP1A1 activity

In an attempt to examine whether the presence of external heme will restore the Hg^{2+}-mediated decrease of CYP1A1 activity, HepG2 cells were co-exposed to 10 μM Hg^{2+} and 1 nM TCDD in the presence and absence of 80 μM hemin, a precursor of heme. Our results showed that hemin alone did not affect CYP1A1 activity. Interestingly, the addition of hemin partially restored the Hg^{2+}-mediated decrease of CYP1A1 activity by 2-fold compared to Hg^{2+} plus TCDD (Fig. 9).

3.10. The effect of HO-1 siRNA on Hg^{2+}-mediated inhibition of CYP1A1 catalytic activity

Despite using selective pharmacological inhibitors such as SnMP and heme precursors like hemin to inhibit HO-1 activity, it was of importance to confirm our hypothesis that the Hg^{2+}-mediated increase in HO-1 is in part responsible for the down-regulation of CYP1A1 at the catalytic activity level. Therefore, we took a genetic approach to confirm whether or not HO-1 is involved in the Hg^{2+}-mediated decrease of the TCDD-mediated induction of CYP1A1 catalytic activity. For this purpose, HepG2 cells were transfected with human HO-1 siRNA for 6 h, and then the cells were treated with 10 μM Hg^{2+} in the presence and absence of 1 nM TCDD. Our results showed that HO-1 siRNA significantly decreased HO-1 mRNA by 0.8-fold as compared to control (Fig. 10A). On the other hand, Hg^{2+} was able to increase HO-1 mRNA levels, in the absence and presence of TCDD, to reach 25-fold compared to control. When the cells were transfected with HO-1 siRNA, and then treated with Hg^{2+} in the presence or absence of TCDD there was a statistically significant decrease in HO-1 mRNA to reach ~4.5-fold compared to control (Fig. 10A). To test the selectivity of the siRNA for HO-1, we determined the CYP1A1 mRNA levels in cells transfected with siRNA for HO-1. Fig. 10B shows that CYP1A1 mRNA levels were not altered by the HO-1 siRNA. Thus, the observed effects on the CYP1A1 catalytic activity levels are solely through knocking-down HO-1.

Looking at CYP1A1 catalytic activity, Hg^{2+} alone or in the presence of HO-1 siRNA did not affect CYP1A1 catalytic activity (Fig. 10C). TCDD alone increased the CYP1A1 catalytic activity by

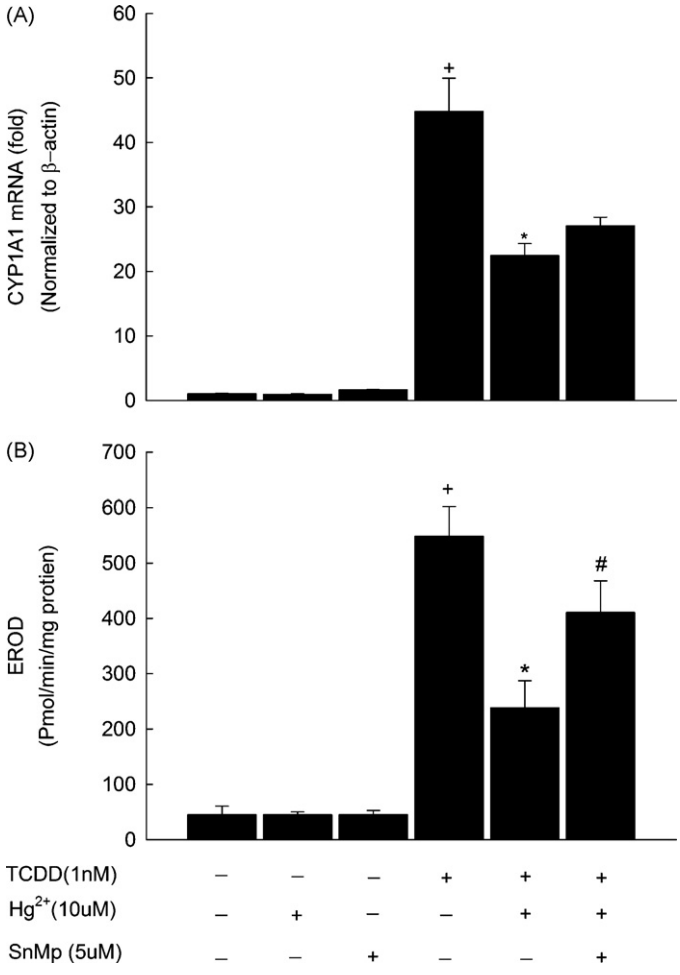

Fig. 8. Effect of SnMP on CYP1A1 mRNA and catalytic activity levels in the presence of Hg^{2+}. HepG2 cells were treated with 10 μM of Hg^{2+} and 1 nM TCDD in the presence and absence of 5 μM SnMP for 6 h for CYP1A1 mRNA, and for 24 h for CYP1A1 catalytic activity. (A) First-strand cDNA was synthesized from total RNA (1 μg) extracted from HepG2 cells. cDNA fragments were amplified and quantitated using ABI 7500 real-time PCR system as described under Section 2. Duplicate reactions were performed for each experiment, and the values presented are the means of six independent experiments ± SE ($n = 6$). (+) $P < 0.05$, compared to control; (*) $P < 0.05$, compared to respective TCDD treatment. (B) CYP1A1 activity was measured using 7-ethoxyresorufin as a substrate. Values are presented as mean ± SE ($n = 8$). (+) $P < 0.05$, compared to control; (*) $P < 0.05$, compared to respective TCDD treatment; (#) $P < 0.05$, compared to respective Hg^{2+} + TCDD treatment.

21-fold, whereas Hg^{2+} significantly decreased the TCDD-mediated induction of CYP1A1 catalytic activity to reach 6-fold compared to control. Interestingly, when HepG2 cells were transfected with HO-1 siRNA and then co-exposed to Hg^{2+} and TCDD, Hg^{2+} decreased the TCDD-induced catalytic activity to reach 17-fold, compared to control, and was unable to maintain the same inhibitory effect on CYP1A1 catalytic activity when compared to non-transfected cells (Fig. 10C).

4. Discussion

Although environmental co-exposures involve both AhR-ligands, typified by TCDD, and heavy metals, typified by Hg^{2+}, the current methods for assessing the potential toxicological consequences are often assuming the additivity of responses. However, this might not be the case, because there is still a possibility of antagonistic or synergistic effect.

In the current study, we examined the potential effect of Hg^{2+} on the TCDD-mediated induction of CYP1A1 gene in human hep-

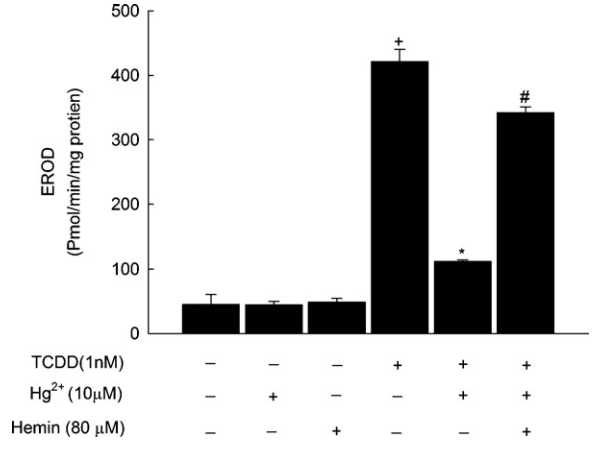

Fig. 9. Effect of supplementing external heme, on Hg^{2+}-mediated decrease of CYP1A1 activity. HepG2 cells were treated with 10 μM Hg^{2+} and 1 nM TCDD in the presence and absence of 80 μM hemin for 24 h. CYP1A1 activity was measured using 7-ethoxyresorufin as a substrate. Values are presented as mean ± SE ($n = 8$). (+) $P < 0.05$, compared to control; (*) $P < 0.05$, compared to respective TCDD treatment; (#) $P < 0.05$, compared to respective Hg^{2+} + TCDD treatment.

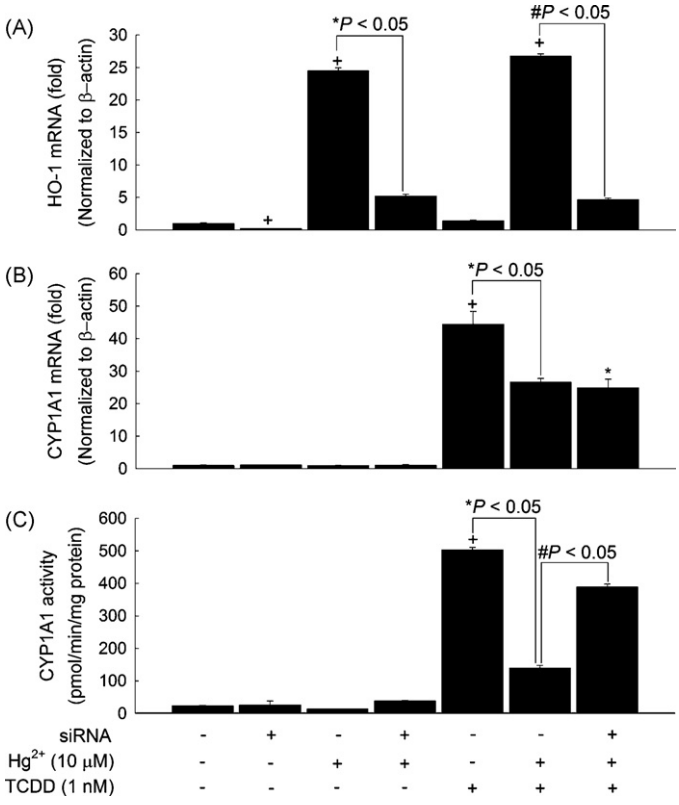

Fig. 10. Effect of HO-1 siRNA on Hg^{2+}-mediated induction of HO-1 mRNA, and Hg^{2+}-mediated inhibition of CYP1A1 mRNA and catalytic activity. HepG2 cells were transiently transfected with 20 nM HO-1 siRNA (siRNA) for 6 h, thereafter cells were treated with vehicle, TCDD (1 nM), Hg^{2+} (10 μM), TCDD (1 nM) + Hg^{2+} (10 μM) for 6 h for HO-1 and CYP1A1 mRNA or 24 h for CYP1A1 protein. (A and B) First-strand cDNA was synthesized from total RNA (1 μg) extracted from HepG2 cells. cDNA fragments were amplified and quantitated using ABI 7500 real-time PCR system as described under Section 2. Duplicate reactions were performed for each experiment, and the values presented are the means of six independent experiments ± SE ($n = 6$). (+) $P < 0.05$, compared to control; (*) $P < 0.05$, compared to respective Hg^{2+} treatment; (#) $P < 0.05$, compared to respective Hg^{2+} + TCDD treatment. (C) CYP1A1 activity was measured using 7-ethoxyresorufin as a substrate. Values are presented as mean ± SE ($n = 6$). (+) $P < 0.05$, compared to control; (*) $P < 0.05$, compared to respective TCDD treatment; (#) $P < 0.05$, compared to respective Hg^{2+} + TCDD treatment.

atoma HepG2 cells. The concentrations of Hg^{2+} utilized in this work were selected based on our cell viability test and previous studies on HepG2 cells (Korashy and El-Kadi, 2008a; Vakharia et al., 2001). These low concentrations of Hg^{2+} used in the current study are within the estimated human plasma and tissue levels in individuals without known exposure (Gerhardsson et al., 1988; Tezel et al., 2001). Taken together, chronic human exposure to these long half-life toxic metals in addition to the high risk of accumulation in the body tissues, particularly the liver (Snow et al., 1989), make the concentrations used in the present study of high relevancy to the corresponding human plasma and tissue levels, and calculated exposure levels in the environment (ATSDR, 2005; CEPA, 2006). The readily available human hepatoma cell line HepG2 was used in the current study for the following reasons: first, the cell line has proven to be a useful model for investigations of the regulations of human CYP1A1 (Kikuchi et al., 1996; Kim et al., 2006; Krusekopf et al., 1997; Lipp et al., 1992; Vakharia et al., 2001); second, the human hepatocyte has been shown to be one of the major targets for heavy metals upon exposure (Ercal et al., 2001).

CYP1A1 gene expression involves the activation of a cytosolic transcriptional factor, the AhR, as the first step in a series of molecular events promoting CYP1A1 transcription and translation processes (Denison et al., 1989). Initially, our results showed that, Hg^{2+} significantly inhibited the TCDD-mediated induction of CYP1A1 at the mRNA, and protein levels at the highest concentration tested which is 10 μM, whereas at the catalytic activity level, Hg^{2+} caused a concentration-dependent inhibition of CYP1A1 (Figs. 2 and 3A). These results are consistent with previously reported observations in HepG2 cells and isolated human hepatocytes showing that Hg^{2+} significantly reduced CYP1A1 induction mediated by benzo[a]pyrene derivatives (Vakharia et al., 2001). In addition, these results are in agreement with our previous observations in human hepatoma HepG2 cells, in that Hg^{2+} at 5 and 10 μM significantly inhibited the induction of the TCDD-mediated induction of CYP1A1 at both protein and catalytic activity levels (Korashy and El-Kadi, 2008a). In contrast, previous data from our laboratory have shown that Hg^{2+} up-regulates *Cyp1a1* gene expression and causes further potentiation of the TCDD-mediated induction of Cyp1a1 mRNA and protein level in murine hepatoma Hepa 1c1c7 cells (Korashy and El-Kadi, 2004, 2005).

The controversy between the effect of Hg^{2+} on the human HepG2 and mouse Hepa 1c1c7 cells could be attributed to the mechanistic differences in the regulation of *CYP1A1* gene expression upon treatment by TCDD (Ramadoss and Perdew, 2005; Ramadoss et al., 2004). Factors that could be responsible for these species-specific characteristics of AhR functions, and subsequently CYP1A1 inducibility, could be summarized in three major components; the nuclear translocation, transcription initiation via remodeling of chromatin, and finally proteasomal degradation of the AhR (Anwar-Mohamed et al., 2009). For example, it has been shown that in Hepa 1c1c7 cells the co-activator CREB-binding protein (CBP) is recruited to the Cyp1a1 promoter region posttreatment with TCDD, reaching its peak at 4 h, and this coincided with the recruitment of AhR and polymerase II, while there was no recruitment of p300 (Suzuki and Nohara, 2007). In contrast, in HepG2, p300 recruitment is increased in response to TCDD to reach its peak between 4 and 12 h, while CBP recruitment is unaffected (Suzuki and Nohara, 2007).

At the transcriptional level, we demonstrated that Hg^{2+} alone or in the presence of TCDD was able to significantly decrease the AhR-dependent luciferase reporter gene expression (Fig. 4). Thus, the down-regulation of *CYP1A1* gene expression by Hg^{2+} was mediated through an AhR-dependant mechanism. Moreover, the ability of Hg^{2+} to decrease the *CYP1A1* gene expression through a transcriptional mechanism prompted further investigation. Therefore, we examined the effect of Hg^{2+} on the CYP1A1 mRNA stability, using Act-D-chase experiment. Our results showed that Hg^{2+} was unable

to significantly alter CYP1A1 mRNA half-life (Fig. 5), implying that Hg^{2+} is mediating its effect through a transcriptional mechanism to inhibit the *CYP1A1* gene expression.

The concentration-dependent decrease of CYP1A1 activity by Hg^{2+} could be attributed, at least in part, to a posttranslational mechanism. Therefore, we examined the effect of Hg^{2+} on the TCDD-mediated induction of CYP1A1 protein half-life using CHX-chase experiments. Our results showed that Hg^{2+} significantly increased CYP1A1 protein degradation rate (Fig. 6), implying the presence of a posttranslational down-regulation of CYP1A1 by Hg^{2+}. In contrast to this finding, we have previously shown that Hg^{2+} increased the TCDD-mediated induction of Cyp1a1 protein stability in Hepa 1c1c7 cells (Korashy and El-Kadi, 2005). These results suggest that the effect of Hg^{2+} on CYP1A1 half-life is species-specific.

In this study, we showed that Hg^{2+} significantly increased the HO-1 mRNA level at all concentrations tested, implying the possibility that Hg^{2+} might have decreased CYP1A1 activity through degrading its heme content via HO-1. HO-1, an enzyme of 32 kDa, catalyzes the oxidative conversion of heme into biliverdin, which serves an important role in protecting cells from oxidative damage, such as free radicals (Marilena, 1997). HO-1 anchors to the endoplasmic reticulum membrane via a stretch of hydrophobic residues at the C-terminus (Schuller et al., 1998). Thus, it is expected to interact with CYP450s which are also endoplasmic reticulum-bound enzymes. The results of the current study are in agreement with our previous published data in which Hg^{2+} was shown to be able to significantly induce HO-1 mRNA expression in Hepa 1c1c7 cells (Korashy and El-Kadi, 2005). The fact that Hg^{2+} induces HO-1 with a consequent decrease in the heme pool could result in the failure to form a functioning CYP1A1 protein. Moreover, the apoprotein would be more susceptible to proteasomal degradation (Anwar-Mohamed et al., 2009).

The role of HO-1 in the down-regulation of CYP1A1 at the catalytic activity level was supported by series of evidence. Firstly, SnMP was able to partially prevent the decrease in TCDD-mediated induction of CYP1A1 activity by Hg^{2+}. The observed effect of SnMP on the Hg^{2+}-mediated decrease of CYP1A1 catalytic activity was solely through competitively inhibiting HO-1 protein and not through altering CYP1A1 mRNA. In addition, it was previously demonstrated that SnMP is incapable of producing any effect on HO-1 mRNA and CYP1A1 mRNA and catalytic activity (Anwar-Mohamed and El-Kadi, 2010). Secondly, we dissected the role of HO-1 in the Hg^{2+}-mediated decrease of CYP1A1 catalytic activity using hemin, a precursor of heme. If Hg^{2+} decreases the TCDD-mediated induction of CYP1A1 activity through degrading its heme, then supplying heme will restore the TCDD-mediated induction of CYP1A1 activity. Interestingly, our results demonstrated that supplying external heme partially prevented the decrease in TCDD-mediated induction of CYP1A1 activity by Hg^{2+}.

Despite using a specific HO-1 inhibitor, SnMP, and heme precursor, hemin, we wanted to confirm the role of HO-1 in the Hg^{2+}-mediated decrease of CYP1A1 catalytic activity using a genetic approach. Our results showed that HO-1 mRNA was successfully knocked-down using HO-1 siRNA in HepG2 cells. Interestingly, Hg^{2+}-mediated decrease in CYP1A1 catalytic activity was partially reversed upon transfection with HO-1 siRNA. To the best of our knowledge this is the first study examining the role of HO-1 in the Hg^{2+}-mediated decrease of CYP1A1 catalytic activity using HO-1 siRNA. Studies from our laboratory and others have shown that in HepG2 cells, HO-1 knock-down partially reverses arsenite-mediated decrease of the TCDD and benzo-k-fluoranthene-induced CYP1A1 catalytic activity level (Anwar-Mohamed and El-Kadi, 2010; Bessette et al., 2009). In addition to HO-1, we have previously reported that activation of NF-κB and/or AP-1 signaling pathways is involved in the modulation of *Cyp1a1* gene expression by heavy metals such as Hg^{2+} in murine hepatoma Hepa 1c1c7 cells (Korashy and El-Kadi, 2008b). Therefore, there is a possibility that NF-κB and AP-1 may directly or indirectly be involved in the modulation of *CYP1A1* expression by Hg^{2+} in human hepatoma HepG2 cells as well.

In conclusion, data presented herein demonstrated for the first time that Hg^{2+} down-regulates the expression of CYP1A1 at transcriptional, and posttranslational levels in HepG2 cells. In addition, Hg^{2+}-mediated induction of HO-1 and CYP1A1 protein degradation are partially involved in the modulation of CYP1A1 at the posttranslational level.

Conflict of interest statement

There are no conflicts of interest.

Acknowledgments

This work was supported by Natural Sciences and Engineering Research Council of Canada (NSERC) Discovery Grant RGPIN 250139-07 to A.O.S. I.E.A is the recipient of Libyan Government Scholarship. A.A-M. is the recipient of Alberta Ingenuity Graduate Scholarship. We are grateful to Dr. M.S. Denison (University of California, Davis, CA) for providing us with XRE-luciferase reporter plasmid pGudLuc 6.1. We would like to thank Dr. W. Todd Rogers (University of Alberta, Canada) for his assistance with statistical analysis.

References

Anwar-Mohamed, A., El-Kadi, A.O., 2009. Sulforaphane induces CYP1A1 mRNA, protein, and catalytic activity levels via an AhR-dependent pathway in murine hepatoma Hepa 1c1c7 and human HepG2 cells. Cancer Letters 275, 93–101.

Anwar-Mohamed, A., El-Kadi, A.O., 2010. Arsenite down-regulates cytochrome P450 1A1 at the transcriptional and posttranslational levels in human HepG2 cells. Free Radical Biology & Medicine 48, 1399–1409.

Anwar-Mohamed, A., Elbekai, R.H., El-Kadi, A.O., 2008. MG-132 inhibits the TCDD-mediated induction of Cyp1a1 at the catalytic activity but not the mRNA or protein levels in Hepa 1c1c7 cells. Toxicology Letters 182, 121–126.

Anwar-Mohamed, A., Elbekai, R.H., El-Kadi, A.O., 2009. Regulation of CYP1A1 by heavy metals and consequences for drug metabolism. Expert Opinion on Drug Metabolism & Toxicology 5, 501–521.

ATSDR, 2005. The Agency for Toxic Substances and Diseases Registry.

Bessette, E.E., Fasco, M.J., Pentecost, B.T., Reilly, A., Kaminsky, L.S., 2009. Investigations of the posttranslational mechanism of arsenite-mediated downregulation of human cytochrome P4501A1 levels: the role of heme oxygenase-1. Journal of Biochemical and Molecular Toxicology 23, 222–232.

CEPA, 2006. Canadian Environmental Protection Act Registry.

Denison, M.S., Fisher, J.M., Whitlock Jr., J.P., 1989. Protein–DNA interactions at recognition sites for the dioxin–Ah receptor complex. Journal of Biological Chemistry 264, 16478–16482.

Elbekai, R.H., El-Kadi, A.O., 2004. Modulation of aryl hydrocarbon receptor-regulated gene expression by arsenite, cadmium, and chromium. Toxicology 202, 249–269.

Elbekai, R.H., El-Kadi, A.O., 2007. Transcriptional activation and posttranscriptional modification of Cyp1a1 by arsenite, cadmium, and chromium. Toxicology Letters 172, 106–119.

Ercal, N., Gurer-Orhan, H., Aykin-Burns, N., 2001. Toxic metals and oxidative stress part I: mechanisms involved in metal-induced oxidative damage. Current Topics in Medicinal Chemistry 1, 529–539.

Gerhardsson, L., Brune, D., Nordberg, G.F., Wester, P.O., 1988. Multielemental assay of tissues of deceased smelter workers and controls. The Science of the Total Environment 74, 97–110.

Gochfeld, M., 2003. Cases of mercury exposure, bioavailability, and absorption. Ecotoxicology and Environmental Safety 56, 174–179.

Hankinson, O., 1995. The aryl hydrocarbon receptor complex. Annual Review of Pharmacology and Toxicology 35, 307–340.

Kikuchi, H., Kato, H., Mizuno, M., Hossain, A., Ikawa, S., Miyazaki, J., Watanabe, M., 1996. Differences in inducibility of CYP1A1-mRNA by benzimidazole compounds between human and mouse cells: evidences of a human-specific signal transduction pathway for CYP1A1 induction. Archives of Biochemistry and Biophysics 334, 235–240.

Kim, W.K., In, Y.J., Kim, J.H., Cho, H.J., Kim, J.H., Kang, S., Lee, C.Y., Lee, S.C., 2006. Quantitative relationship of dioxin-responsive gene expression to dioxin response element in Hep3B and HepG2 human hepatocarcinoma cell lines. Toxicology Letters 165, 174–181.

Korashy, H.M., El-Kadi, A.O., 2004. Differential effects of mercury, lead and copper on the constitutive and inducible expression of aryl hydrocarbon receptor (AHR)-regulated genes in cultured hepatoma Hepa 1c1c7 cells. Toxicology 201, 153–172.

Korashy, H.M., El-Kadi, A.O., 2005. Regulatory mechanisms modulating the expression of cytochrome P450 1A1 gene by heavy metals. Toxicological Sciences 88, 39–51.

Korashy, H.M., El-Kadi, A.O., 2008a. Modulation of TCDD-mediated induction of cytochrome P450 1A1 by mercury, lead, and copper in human HepG2 cell line. Toxicology In Vitro 22, 154–158.

Korashy, H.M., El-Kadi, A.O., 2008b. The role of redox-sensitive transcription factors NF-kappaB and AP-1 in the modulation of the Cyp1a1 gene by mercury, lead, and copper. Free Radical Biology & Medicine 44, 795–806.

Krusekopf, S., Kleeberg, U., Hildebrandt, A.G., Ruckpaul, K., 1997. Effects of benzimidazole derivatives on cytochrome P450 1A1 expression in a human hepatoma cell line. Xenobiotica 27, 1–9.

Lipp, H.P., Schrenk, D., Wiesmuller, T., Hagenmaier, H., Bock, K.W., 1992. Assessment of biological activities of mixtures of polychlorinated dibenzo-p-dioxins (PCDDs) and their constituents in human HepG2 cells. Archives of Toxicology 66, 220–223.

Lorenzen, A., Kennedy, S.W., 1993. A fluorescence-based protein assay for use with a microplate reader. Analytical Biochemistry 214, 346–348.

Marilena, G., 1997. New physiological importance of two classic residual products: carbon monoxide and bilirubin. Biochemical and Molecular Medicine 61, 136–142.

McLemore, T.L., Adelberg, S., Liu, M.C., McMahon, N.A., Yu, S.J., Hubbard, W.C., Czerwinski, M., Wood, T.G., Storeng, R., Lubet, R.A., et al., 1990. Expression of CYP1A1 gene in patients with lung cancer: evidence for cigarette smoke-induced gene expression in normal lung tissue and for altered gene regulation in primary pulmonary carcinomas. Journal of the National Cancer Institute 82, 1333–1339.

Meyer, B.K., Pray-Grant, M.G., Vanden Heuvel, J.P., Perdew, G.H., 1998. Hepatitis B virus X-associated protein 2 is a subunit of the unliganded aryl hydrocarbon receptor core complex and exhibits transcriptional enhancer activity. Molecular and Cellular Biology 18, 978–988.

Nebert, D.W., Dalton, T.P., Okey, A.B., Gonzalez, F.J., 2004. Role of aryl hydrocarbon receptor-mediated induction of the CYP1 enzymes in environmental toxicity and cancer. Journal of Biological Chemistry 279, 23847–23850.

Ramadoss, P., Perdew, G.H., 2005. The transactivation domain of the Ah receptor is a key determinant of cellular localization and ligand-independent nucleocytoplasmic shuttling properties. Biochemistry 44, 11148–11159.

Ramadoss, P., Petrulis, J.R., Hollingshead, B.D., Kusnadi, A., Perdew, G.H., 2004. Divergent roles of hepatitis B virus X-associated protein 2 (XAP2) in human versus mouse Ah receptor complexes. Biochemistry 43, 700–709.

Schuller, D.J., Wilks, A., Ortiz de Montellano, P., Poulos, T.L., 1998. Crystallization of recombinant human heme oxygenase-1. Protein Science 7, 1836–1838.

Shimada, T., Fujii-Kuriyama, Y., 2004. Metabolic activation of polycyclic aromatic hydrocarbons to carcinogens by cytochromes P450 1A1 and 1B1. Cancer Science 95, 1–6.

Snow, R.C., Barbieri, R.L., Frisch, R.E., 1989. Estrogen 2-hydroxylase oxidation and menstrual function among elite oarswomen. The Journal of Clinical Endocrinology and Metabolism 69, 369–376.

Suzuki, T., Nohara, K., 2007. Regulatory factors involved in species-specific modulation of arylhydrocarbon receptor (AhR)-dependent gene expression in humans and mice. Journal of Biochemistry 142, 443–452.

Tezel, H., Ertas, O.S., Erakin, C., Kayali, A., 2001. Blood mercury levels of dental students and dentists at a dental school. British Dental Journal 191, 449–452.

Vakharia, D.D., Liu, N., Pause, R., Fasco, M., Bessette, E., Zhang, Q.Y., Kaminsky, L.S., 2001. Polycyclic aromatic hydrocarbon/metal mixtures: effect on PAH induction of CYP1A1 in human HEPG2 cells. Drug Metabolism and Disposition: The Biological Fate of Chemicals 29, 999–1006.

Whitelaw, M.L., Gustafsson, J.A., Poellinger, L., 1994. Identification of transactivation and repression functions of the dioxin receptor and its basic helix-loop-helix/PAS partner factor Arnt: inducible versus constitutive modes of regulation. Molecular and Cellular Biology 14, 8343–8355.

Zalups, R.K., 2000. Molecular interactions with mercury in the kidney. Pharmacological Reviews 52, 113–143.